

## Imaging Pyrometry of Laser-Heated Sapphire

*David H. Terry, Michael E. Thomas, Milton J. Linevsky, and Daniel T. Prendergast*

A long-wave infrared camera was used in an imaging pyrometric mode to determine the spatially resolved outer surface temperature of sapphire samples heated with a carbon dioxide (CO<sub>2</sub>) laser. Tests were conducted by APL at the Laser Hardened Materials Evaluation Laboratory, Wright-Patterson Air Force Base, Ohio. Sapphire disks were assessed first to demonstrate the CO<sub>2</sub> laser heating technique and the capabilities of the infrared pyrometry system. Additional testing was conducted on sapphire domes that are candidates for infrared seeker windows. The laser heating profile presented (written) to each dome during testing simulated the aerothermal heating profiles that were observed in hypersonic wind tunnel tests conducted in APL's Advanced Technology Development Laboratory. Only sapphire disk test results are presented here, although both disk and dome testing protocols are discussed. (Keywords: Infrared imaging pyrometry, Infrared thermometry, Laser heating, Sapphire properties.)

### INTRODUCTION

APL has developed a method of measuring the surface temperatures of oxide window materials by employing a long-wave infrared (LWIR) mercury-cadmium-telluride (MCT) camera (Thermovision Model 1000, manufactured by AGEMA). The camera yields spatially resolved (400 × 800 pixel) measurements of the temperature increase of a sapphire disk or dome as it undergoes heating. The two-dimensional images from the camera provide a radiometrically calibrated method of determining the temperature across the outer surface of sapphire. This article describes the results of carbon dioxide (CO<sub>2</sub>) laser heating tests conducted by APL in early 1998. The thermal images that were obtained of sapphire disks during these tests further demonstrate

the principle of this temperature measurement system. The dome tests, performed by APL at the Laser Hardened Materials Evaluation Laboratory (LHMEL), Wright-Patterson Air Force Base, Ohio, also demonstrated the similarity between previous wind tunnel aerothermal heating tests and these CO<sub>2</sub> laser heating tests.

One of the many critical issues in the development of an infrared seeker for tactical missile applications is obtaining material properties of its window. A sapphire dome will undergo a significant increase in temperature due to aerodynamic heating during missile flight. APL's Advanced Technology Development Laboratory (ATDL) Test Cell 4 wind tunnel<sup>1</sup> has been used extensively over

the past decade to simulate flight conditions for a variety of missiles, windows, and domes, including (most recently) sapphire domes.<sup>2</sup> Critical questions (e.g., the proper orientation of the sapphire dome's crystalline structure with respect to the missile body) have been answered through the ATDL research, thus ensuring a greater likelihood of dome survivability during flight.

An important aspect of wind tunnel measurements is the temperature data obtained by thermocouples. An imaging pyrometry system<sup>3</sup> was therefore developed to enhance existing thermocouple data collection methods by providing noncontact thermal imaging of the outer surface of sapphire test articles during aerothermal heating.

Although wind tunnel tests are useful for characterizing the effects of aerothermal heating on sapphire, other questions could be answered in a more optically benign environment than that of a turbulent wind tunnel flow. For example, tests of the amount of bore-sight error that is caused by the sapphire window's temperature increase can be measured through interferometry. Also, the internal stresses and strains caused by the heating of sapphire's crystalline lattice can be measured through polarization techniques. Such tests are best conducted in environments where any observed effect is due solely to sapphire heating and not to any optical path effects such as turbulence. Therefore, the CO<sub>2</sub> laser heating of sapphire was studied to simulate the aerothermal heating profiles measured at APL.

The imaging pyrometry system previously used during wind tunnel measurements was modified to support measurements of laser-heated sapphire disks and domes at the LHMEF facility. The characterization of the optical property of single-crystal sapphire conducted 7 to 13 years ago at APL<sup>4-7</sup> provided a database to support remote sensing of the surface temperature of sapphire. Noninvasive measurements of temperature were sought to replace thermocouples attached to the inside surface of these domes.

Imaging pyrometry works optimally when the material under analysis behaves as a blackbody. For materials with infrared-active lattice vibrations, the two-phonon region most closely resembles a blackbody. The two-phonon spectral interval extends from the maximum longitudinal vibration frequency of the insulator to roughly 1.8 times that frequency (the upper limit will depend on the material thickness). For the ordinary ray (o-ray) of sapphire, the spectral region extends from 914 to 1645 cm<sup>-1</sup>. This interval is illustrated for the sapphire o-ray in Fig. 1, which plots the near-normal experimental emittance spectrum as a function of temperature.<sup>7</sup> Note that within the two-phonon region, the emittance is close to 1 and virtually independent of the sample temperature.

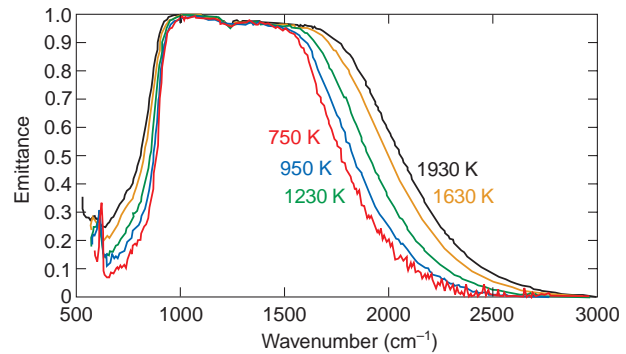


**Figure 1.** Near-normal emittance of a 1-mm-thick sapphire o-ray at various temperatures.

Another property of sapphire in this region is high absorption. Therefore, the material is opaque and the reflectance is very low. The index of refraction is close to 1 in the two-phonon region (a result of anomalous dispersion), and thus the unpolarized Fresnel power reflection coefficient is close to zero. Furthermore, since the reflection coefficient is small, the weak temperature dependence of the index of refraction makes the emittance virtually temperature independent. This point is illustrated in Fig. 2 for sapphire.

An additional important consequence of the complex index of refraction in the two-phonon region is that the Fresnel reflection coefficient is constant with angle out to near-oblique angles. This point is illustrated in Fig. 3. The figure plots the computed emittance of sapphire o-ray at 600 K as a function of angle  $\theta$  for two different wavenumbers  $\nu$ . The real and imaginary parts of the complex index of refraction,  $n$  and  $k$ , respectively, depend on wavenumber and are  $n = 0.867$  and  $k = 0.063$  (for  $\nu = 1000$  cm<sup>-1</sup>) and  $n = 1.264$  and  $k = 0.024$  (for  $\nu = 1200$  cm<sup>-1</sup>). Therefore, sapphire samples can be viewed at angles from 0 to approximately 60° without significant changes in directional emissivity. This property of the directional emissivity,

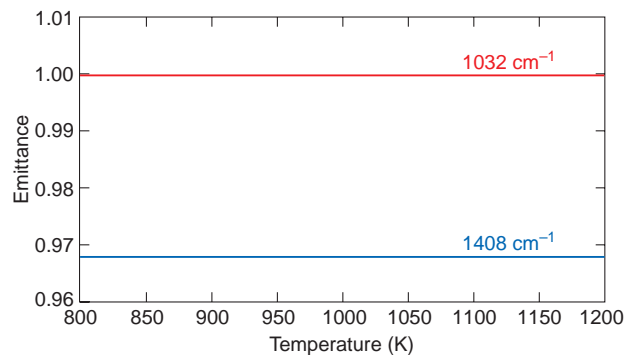


**Figure 2.** Temperature dependence of the emittance of sapphire o-ray at two spectral points within the two-phonon region.

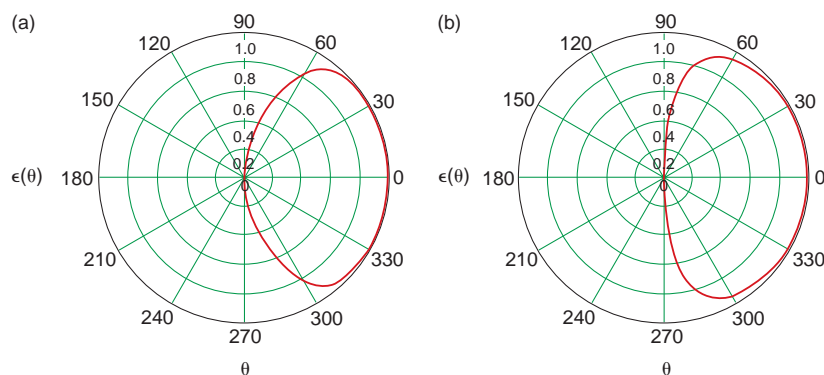


**Figure 3.** Plots of the directional emittance,  $\epsilon(\theta)$ , of sapphire o-ray at 600 K as a function of angle  $\theta$  demonstrating the near Lambertian character: (a) at  $1000\text{ cm}^{-1}$ , where the real part of the complex index of refraction  $n = 0.867$  and the imaginary part  $k = 0.063$ , and (b) at  $1200\text{ cm}^{-1}$ , where  $n = 1.264$  and  $k = 0.024$ .

combined with the near-blackbody properties and near-temperature independence of sapphire, make the two-phonon region an excellent band for measuring the outer surface temperatures of sapphire windows. Thus, a pyrometry system with a passband in the LWIR (7.4 to  $11.7\text{ }\mu\text{m}$ ) is used. Figure 4 shows the emittance of sapphire at 700 K in this band.

## CAMERA SYSTEM

The MCT LWIR camera used to collect laser heating measurements at LHMEI contained some refractive germanium collecting optics, reflective scanning optics, and five SPRITE (signal-processing-in-the-element) detectors, which were cooled to 80 K by a Stirling closed-cycle minicooler. The camera has both a wide and narrow field of view (FOV) set of collecting optics which can be used interchangeably (the two lens systems rotate about an axis within the camera housing). The wide FOV set of lenses is used for imaging pyrometry work, providing angular coverage of  $20 \times 13.3^\circ$  and an instantaneous FOV of 0.6 mrad per pixel.

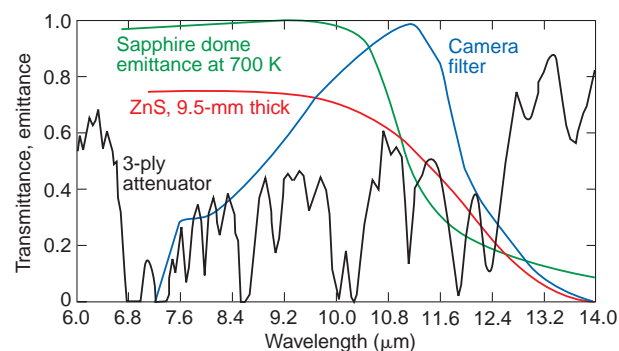


**Figure 4.** Spectral response functions of various components in the pyrometer system.

Both analog and digital outputs were obtained from the LWIR camera. The analog output was standard 30-Hz video and was recorded directly to videotape, which could be subsequently digitized to 8 bits of pixel resolution. The digital output was of higher quality since it had a 12-bit dynamic range, but it was obtained at a much slower rate of approximately 1.1 Hz (period of about 0.88 s).

The camera system underwent four modifications from its original factory specifications. First, a long wavelength pass (low frequency pass) cold filter was added to the

internal optics by AGEMA to reduce the infrared band responsivity from the original 4 to  $14\text{ }\mu\text{m}$  band (which incorporated some mid-wave responsivity) to the LWIR band of 7.4 to  $14\text{ }\mu\text{m}$ . The camera's passband is depicted in Fig. 4.

Since the aim was to measure temperatures of sapphire greater than 400 K, and since the camera in its original configuration saturated near that temperature (approximately 400 K), a second modification to the camera was required. APL constructed an external iris and attenuator system to reduce the amount of energy incident on the SPRITE detectors. The iris was kept at a constant aperture diameter of 2.48 cm (reduced from 10.16 cm), and the attenuator material was a 3-ply plastic (a commercially available viewgraph sleeve) that was approximately 30% transmissive in the LWIR. By incorporating three layers of the attenuator material, the LWIR camera's temperature range was extended beyond 775 K. The spectral characteristics of the 3-ply attenuator are also shown in Fig. 4.

A third change, required when measuring  $\text{CO}_2$  laser-heated samples, was the addition of a sulfur hexafluoride ( $\text{SF}_6$ ) absorption cell. This cell provided an optical density of 6 to 7 at  $10.6\text{ }\mu\text{m}$ , thus absorbing any  $\text{CO}_2$  radiation that reflected off the sapphire sample's surface. The camera could record such radiation because it is sensitive to  $10.6\text{ }\mu\text{m}$ . Also, the absorption cell protected the camera from possible damage due to inadvertent laser reflection. The  $\text{SF}_6$  cell had a barium fluoride ( $\text{BaF}_2$ ) window on each end, and the spectrally varying transmittance of the  $\text{SF}_6$  cell and its two  $\text{BaF}_2$  windows were factored into the camera's calibration. Figure 5 shows the transmittance of the  $\text{SF}_6$  cell as a function of wavelength.

The fourth change to the camera system was the inclusion of a strontium fluoride ( $\text{SrF}_2$ ) window between the  $\text{SF}_6$  cell and the plastic 3-ply attenuator material. The  $\text{SrF}_2$  window acted as a high-frequency

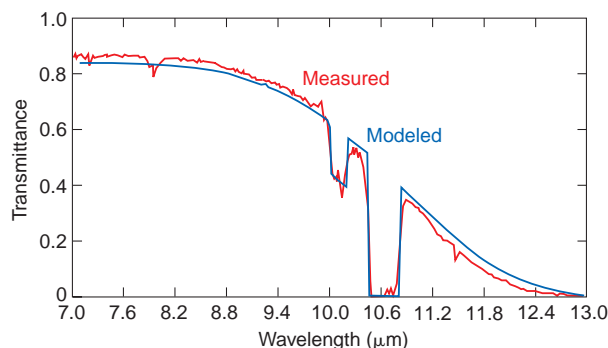


**Figure 5.** Modeled and measured transmittance of the SF<sub>6</sub> cell notch filter for a path of 10 cm (SF<sub>6</sub> partial pressure = 19 Torr plus 741 Torr nitrogen).

pass filter (long-wavelength cutoff) at 11.7 μm. This window further narrowed the pyrometry system's pass-band so that it corresponded closely to the two-phonon region (7 to 11 μm) where sapphire emits like a blackbody. The band-averaged emittance of sapphire over the response band of the camera thus became 0.947.

## CALIBRATION PROCEDURE

The camera was calibrated from 325 to 775 K by taking blackbody measurements at 50 K intervals through that temperature range. One key aspect to the uniqueness of this approach is that the measurement relies on the use of a blackbody to calibrate the digital counts over the temperature range of interest, rather than using a thermocouple to establish the calibration. Furthermore, the number of plies of attenuator material can be increased (or reduced) to measure higher (or lower) temperature ranges if so desired. Changing the number of plies would require another set of calibration measurements with the blackbody. For the purposes of the sapphire disk and dome measurements made at the LHMEF facility, a 3-ply attenuator configuration was used.

For this procedure, a variable-temperature blackbody cavity is viewed by the camera matching the optical path of the experiment and the electronic recording equipment. The average number of counts is determined over the center of the blackbody image as a function of temperature. The measured counts are then converted to radiance. The theoretical blackbody spectral radiance  $L_{bb}(\nu, T)$ , in watts  $\text{cm}^{-2} \text{sr}^{-1} \text{cm}$ , is used in calibration to determine the band-averaged computed radiance,

$$L_{\text{computed}}(T) = \int_{600}^{1350} L_{bb}(\nu, T) \text{SRF}(\nu) d\nu \quad \text{W}/(\text{cm}^2 \cdot \text{sr}), \quad (1)$$

where  $\text{SRF}(\nu)$  is the system response function,  $T$  is temperature in Kelvin, and  $\nu$  is wavenumber in  $\text{cm}^{-1}$ . Determining  $\text{SRF}(\nu)$  requires the mathematical representation of the spectral transfer of all the components in the optical path. For the LHMEF tests, the system response function included the camera response function  $\text{CRF}(\nu)$ , attenuators  $a(\nu)$ , and the transmittance of several windows, i.e., the zinc sulfide (ZnS) vacuum chamber window transmittance,<sup>8</sup> SF<sub>6</sub> cell (with BaF<sub>2</sub> windows) transmittance, and SrF<sub>2</sub> window transmittance  $\tau(\nu)$ . The spectral emittance  $\epsilon(\nu, T)$  of the object (in this case, sapphire) must also be known. The spectral responses are plotted in Fig. 4. In terms of the system components, the system response function becomes

$$\text{SRF}(\nu) = \text{CRF}(\nu)[a(\nu)][\tau(\nu)]. \quad (2)$$

The  $\text{CRF}(\nu)$  comes from a curve obtained from the manufacturer and a cutoff filter at 7.4 μm. A piecewise continuous, functional representation is generated by curve-fitting various spectral regions. Various thicknesses of plastic film are used to obtain different degrees of attenuation. Although the plastic film attenuator is highly variable in frequency, the somewhat regular structure produces a constant attenuation factor. This is useful in reducing computation time during the calibration analysis. The window on the vacuum chamber is 0.95-cm-thick ZnS with a viewing angle near normal. For sapphire, a long-wavelength cutoff of 11 μm is desirable to avoid the low-emittance, temperature-dependent one-phonon region (see Fig. 4).

The ability to compute the measured blackbody radiance allows direct conversion of counts to radiance. This is accomplished by a least-squares linear fit of measured camera counts to the computed radiance as specified by Eq. 1. The resulting formula is given by

$$L_{\text{measured}}(T) = \frac{\text{Counts}(T) - \alpha}{\beta}, \quad (3)$$

where  $\alpha$  is the camera background and  $\beta$  is a scaling factor to obtain radiance in  $\text{W}/(\text{cm}^2 \cdot \text{sr})$ . For the most recent laser-heating sapphire disk and dome measurements with the pyrometry system, the values were  $\alpha = 931$  and  $\beta = 3.1353 \times 10^5$ .

The agreement between the measured and computed radiance as a function of temperature was very good. A typical plot is shown in Fig. 6. The computation of radiance is accomplished in two ways. The first is to numerically solve Eq. 1. The second approach assumes that the attenuator is spectrally uniform and can be



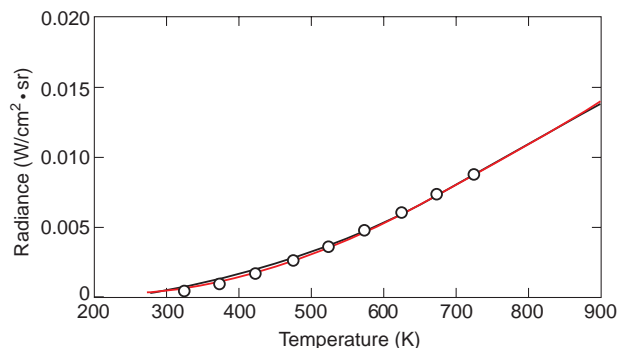


**Figure 6.** Measured (open circles) and modeled band radiance as a function of temperature for a blackbody (red curve: band-integrated radiance with spectrally constant attenuator; black curve: band-integrated radiance with spectrally dependent attenuator).

removed from the integrand to become a constant factor multiplying the integral. This assumption greatly reduces the computation time of numerically solving Eq. 1. The close agreement between the two curves proves that this approximation is valid.

The last step is to compute the temperature. This is accomplished by equating the measured radiance (Eq. 3) to the computed radiance (Eq. 1). In general, the inversion of this complicated equation is not tractable. However, we have found the following function to accurately fit the computed radiance as given by Eq. 1:

$$L_{\text{fit}}(T) = \exp(a + b/T + c/T^2), \quad (4)$$

where  $a = -2.496$ ,  $d = b/c = -0.0293$ , and  $c = 6.5817 \times 10^4$ . This functional form allows a tractable solution for temperature, knowing the band-limited blackbody radiance of the target, as given by

$$T = \frac{2}{-d - (d^2 - 4\{a - \ln[L_{\text{measured}}(T)]\}/c)^{1/2}}. \quad (5)$$

If the radiance is known with certainty, the accuracy of the radiometrically determined temperature is  $\pm 2$  K. Equation 3 is used to determine the measured blackbody radiance.

The practical application of imaging pyrometry usually requires the remote measurement of the temperature of a non-blackbody surface. Thus, the spectral and spatial aspects of the target must be known. Corrections for the non-blackbody character must be incorporated into Eq. 5.

The spectral correction factor is determined by the band-averaged emittance,

$$\epsilon(T) = \frac{\int L_{\text{bb}}(\nu, T)\epsilon(\nu, T)\text{SRF}(\nu) d\nu}{\int L_{\text{bb}}(\nu, T)\text{SRF}(\nu) d\nu}. \quad (6)$$

Optimally, the band-averaged emittance is temperature insensitive, which is true for sapphire from 7 to 11  $\mu\text{m}$ . Since the modified camera system operates from 7.4 to 11.7  $\mu\text{m}$ , there is a weak temperature dependence in the sapphire emittance over the temperature range of interest. However, because this effect is small, no attempt to compensate for temperature dependence was made. In Eq. 5, the target is assumed to be a blackbody. For a non-blackbody target,  $L_{\text{measured}}$  in Eq. 5 must be replaced by  $L_{\text{measured}}/\epsilon$ , where  $\epsilon = 0.947$ . It is also assumed that the target is in thermal equilibrium and Lambertian, and that the emittance is independent of temperature. Although this imaging pyrometry calibration approach requires more work than other schemes, it allows accurate extrapolation to room temperature by the calibration formula and validates the quality of the calibration measurements on the blackbody.

## LWIR IMAGING PYROMETER OPERATION

The camera settings (focus, integration time, etc.) were changed through a series of on-screen set-up menus displayed on the camera's analog output channel. The camera could also be controlled by a laptop computer over the same digital communications link that transfers the digital image frames. During a test, the camera operator sequentially triggered the collection of images by using AGEMA control software.

The resulting set of images was taken, on average, 0.88 s apart (for a digital frame rate of about 1.1 Hz). The timing of the frames was aperiodic, probably due to a combination of communications link synchronization and the multitasking environment of the operating system. As a result, various changes in computer resource allocation (CPU time) were made while the AGEMA camera control software was operating. The timing of each image was extracted from a time stamp (an encoded series of bytes) that followed the pixel data within each digital file. The time stamp provides time resolution to a hundredth of a second.

The complete LWIR imaging pyrometry system is portable, as evidenced by our field tests at LHMEI (mid-1997 and, most recently, in early 1998). The camera, power supply, and remote control are contained in one carrying case. A collapsible tripod is used for mounting the camera. The PC laptop, its docking station, and Bernoulli removable disk drives form the operator control station, which can be located as far as

30 m from the camera through extra-long cables obtained for the tests at ATDL. A video cassette recorder and monitor are used to record and view the analog channel from the camera, and a four-channel date/time character generator allows synchronization of the LWIR video channel with the video channels of other sensors.

## RESULTS

For the most recent test (Test 36) at LHMEI, the 6.5-cm-dia.  $\times$  2.6-mm-thick sapphire disk was mounted inside a vacuum chamber, which was pumped down to approximately  $10^{-4}$  Torr. The  $\text{CO}_2$  laser was typically operated between 1 and 2 kW. The laser was split into two beams: a flood beam and a scan beam. The flood beam was designed to have a diameter approximately equal to the diameter of the sapphire dome ( $\approx 9.65$  cm) and was intended to heat most of a dome's outer surface. The scan beam was more concentrated, with a hot spot written onto the leading edge of the dome.

For dome tests, the scan beam was dithered along the horizontal axis at a rate of 11 Hz, producing an elongated, elliptical hot spot across the dome, analogous to the hot spot produced during wind tunnel tests. For disk tests, the scan beam was not dithered, since the disk samples were smaller in diameter than the dome samples. Thus, for disk tests, the scan beam presented a smaller hot spot in the center of the disk. The laser had a top-hat beam intensity profile that was masked with a neutral density aperture ring to reduce any sharp gradients of the beam edges. As depicted in Fig. 7, the scan beam heated the sapphire sample by entering a

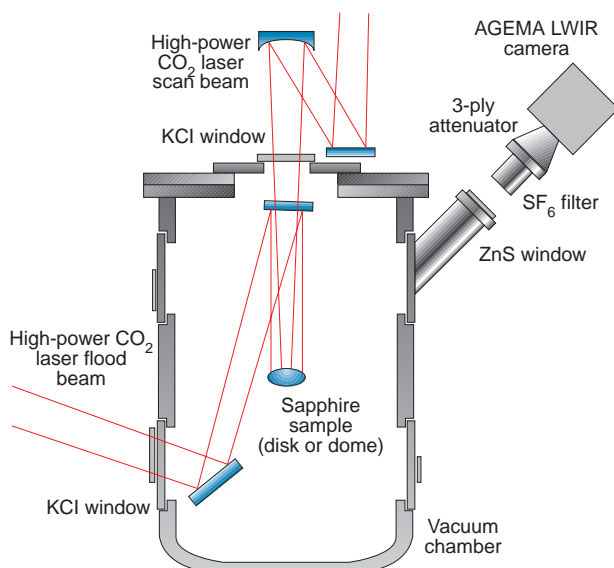


**Figure 7.** Experiment setup at the LHMEI facility showing the alignment of the laser flood and scan beams onto a sapphire sample relative to the LWIR imaging pyrometry system.

potassium chloride (KCl) window in the front of the vacuum chamber. The scan beam then illuminated a disk at a near-normal angle, and illuminated a dome between its crown and edge. The flood beam was brought in through a side window of the vacuum chamber and was reflected with mirrors onto the sample at about a  $25^\circ$  angle in the vertical plane, relative to the scan beam.

To analyze, in a calibrated manner, the surface temperature of sapphire as it warms owing to laser heating, the digital frames were converted from pixel counts to radiance and then to temperature. Twenty-four digital frames were acquired during the short-duration tests at a rate of 1.1 Hz. Usually the first two or three images were collected before the laser shutter was opened, four or five images were collected during a typical 4-s heating exposure, and the remainder were collected during cooldown after the laser shutter was closed. Each digital image was made up of 400 rows and 800 columns of pixels, and each pixel was rectangular, with a 3 to 4 aspect ratio between the vertical and horizontal. The horizontal axis had to be scaled by 0.75 to bring the images into proper perspective to prevent circular objects from appearing elliptical. The pixels were converted to radiances by Eq. 3, and the radiances were converted into temperatures using Eq. 5.

The pyrometry system was mounted on a tripod outside the LHMEI vacuum chamber, and the sapphire sample was observed through a  $45^\circ$  angle viewport. Thus, the pyrometry system imaged both the front and side of the sample during a test.

Examples of some measurements are shown in Fig. 8 for Test 36. Each image was a  $120 \times 120$  pixel sub-image of the original  $400 \times 800$  image. For the disk measurement shown in Fig. 8, the first five subimages were collected while the laser shutter was open and the disk was being actively heated for 4 s. Since the disk was viewed from the side at an angle of approximately  $48^\circ$ , the imagery was re-scaled by  $\cos(48^\circ)$  along the horizontal axis to make the disks look circular. The time listed under each subimage in Fig. 8 is relative to the opening of the laser shutter ( $t = 0$ ). The remaining seven images correspond to the period immediately after the shutter was closed and the disk began cooldown. The maximum temperature in this disk measurement was 470 K, which was observed at the hot spot of the fifth subimage (last frame where the laser shutter was still open).

The imagery provided by the pyrometry system is analogous to having a thermocouple located on the outer surface of the sapphire at each pixel of the disk or dome sample. Obviously, a thermocouple cannot be placed on the outer surface without affecting the experiment. Therefore, the pyrometry system offers a direct, noninvasive measurement of the outer surface temperature. Furthermore, the LWIR pyrometry system

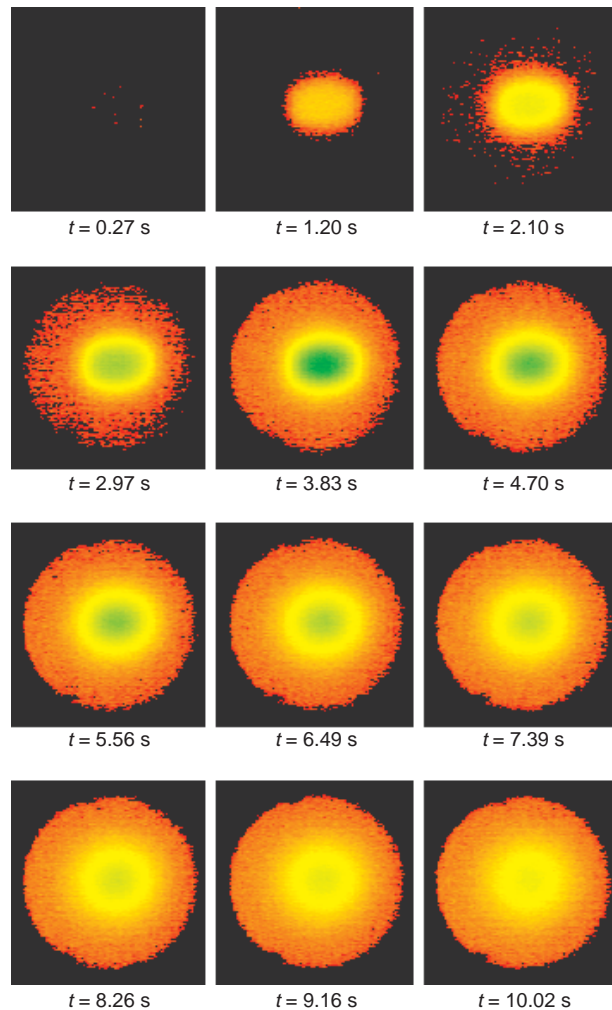


**Figure 8.** Images of a laser-heated sapphire disk (Test 36). Images are corrected for 48° viewing angle. The laser was heating the disk during the first five images (4-s exposure time  $t$ ). Cooldown occurred during the last seven images.

yields two-dimensional data of the temperature over the entire surface of the dome or disk. Thus, the spatially resolved imagery allows one to study the diffusion of heat from the hot spot toward the edge of the disk or dome during laser heating. Such diffusion can be seen in the later frames of Fig. 8 where the edge of the disk is clearly distinguishable. This example illustrates

the pyrometric technique for sapphire disks. Results from additional disk<sup>9,10</sup> and dome tests<sup>10</sup> are available elsewhere.

## SUMMARY

The use of a scanning MCT LWIR camera to measure the outer surface temperature of sapphire during laser heating has been shown to be a valuable diagnostic tool that is preferable to thermocouples. The results of these sapphire measurements made at the LHMEL facility with the LWIR imaging pyrometry system indicate that this approach provides a valuable noninvasive, calibrated method of measuring the outer surface temperatures of sapphire as it is laser heated to simulate missile flight environments. Combined with other optical techniques for measuring material stresses and boresight errors, the system provides an important diagnostic capability for understanding the properties of sapphire windows used in infrared seekers.

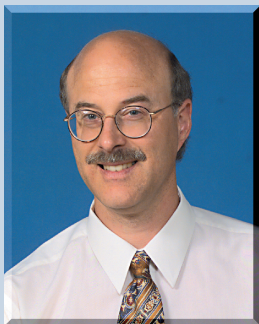
## REFERENCES

- <sup>1</sup>Sullins, G. A., Frazer, R. K., and Neuenhoff, M. J., "Capabilities of the Johns Hopkins University Applied Physics Laboratory Aerothermal Infrared Test Facility," in *Proc. 3rd Annual AIAA/BMDO Interceptor Technology Conf.*, (available through DTIC), San Diego, CA (Jul 1994).
- <sup>2</sup>Sullins, G. A., and Neuenhoff, M. J., "Testing at the Johns Hopkins University Applied Physics Laboratory High-Speed Aerothermal Test Facility," in *Proc. 6th DoD Electromagnetic Windows Symp.*, Redstone Arsenal, AL, pp. 244–251 (Oct 1995).
- <sup>3</sup>Terry, D. H., and Thomas, M. E., "Imaging Pyrometry of Sapphire Domes," in *Proc. 6th Annual AIAA/BMDO Interceptor Technology Conf.*, (available through DTIC), San Diego, CA (Aug 1997).
- <sup>4</sup>Thomas, M. E., Joseph, R. I., and Trof, W. J., "Infrared Transmission of Sapphire, Spinel, Yttria and ALON as a Function of Temperature and Frequency," *Appl. Opt.* 17(2), 239–245 (1988).
- <sup>5</sup>Hoffmann, C. E., Thomas, M. E., and Joseph, R. I., *Optical Constants of Infrared Active Phonons as a Function of Frequency and Temperature*, TG 1376, JHU/APL, Laurel, MD (Nov 1989).
- <sup>6</sup>Thomas, M. E., "The Infrared Properties of the Extraordinary Ray Multiphonon Processes of Sapphire," *Appl. Opt.* 28, 3277–3278 (1989).
- <sup>7</sup>Sova, R. M., Linevsky, M. J., Thomas, M. E., Joseph, R. I., and Mark, F. F., "High Temperature Optical Properties of Oxide Dome Materials," *Johns Hopkins APL Tech. Dig.* 13(3), 368–378 (1992).
- <sup>8</sup>Trof, W. J., Thomas, M. E., and Harris, T. J., "Optical Properties of Crystals and Glasses," Chapter 33 in *Handbook of Optics, Vol. 2: Optical Materials and Properties*, 2nd Ed., The Optical Society of America, McGraw-Hill, New York (1995).
- <sup>9</sup>Thomas, M. E., Wayland, P. S., and Terry, D. H., "Imaging Pyrometry of Oxides," *Proc. SPIE-Thermosense XX* 3361, 2–13 (Apr 1998).
- <sup>10</sup>Terry, D. H., Thomas, M. E., Linevsky, M. J., Prendergast, D. T., Bagford, J. O., and Lander, M. L., "Imaging Pyrometry of Laser-Heated Sapphire," in *Proc. 7th DoD Electromagnetic Windows Symp.*, JHU/APL, Laurel, MD, pp. 264–276 (May 1998).

## THE AUTHORS



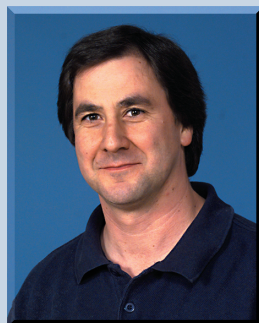
DAVID H. TERRY is a Senior Professional Staff engineer in APL's Electro-Optical Systems Group of the Air Defense Systems Department. He received a B.S.E.E. in electrical engineering and computer science from The Johns Hopkins University in 1987. He has also received an M.S.E. in electrical and computer engineering (1987), an M.S. in applied mathematics (1989), and an M.S. in applied physics (1992), all from JHU. Since joining APL in 1987, he has worked on a variety of tasks including neural network ship classification, a multi-aperture optical correlator (patented in 1998), and the calibration of MSX spacecraft optical sensors. Most recently he has been working on infrared imaging, including the pyrometry of sapphire and the characterization of Theater Ballistic Missile Defense target signatures. His e-mail address is david.terry@jhuapl.edu.



MICHAEL E. THOMAS received a B.E.E. from the University of Dayton, and M.S. and Ph.D. degrees from Ohio State University. Since joining APL in 1979, his work has focused on electromagnetic propagation and optical properties of materials. In 1982, he was a post-doctoral fellow in the Department of Physics, Naval Postgraduate School. In 1988, Dr. Thomas became a faculty member of the JHU G.W.C. Whiting School of Engineering Part-Time Programs in Engineering and Applied Science, teaching courses on optical propagation and lasers. In 1998, he was appointed Research Professor in the Department of Electrical and Computer Engineering at JHU. His current research interests include experimental and theoretical modeling of atmospheric propagation in the infrared, lidar, optical and infrared window materials, and the infrared properties of high-pressure gases. His e-mail address is michael.thomas@jhuapl.edu.



MILTON J. LINEVSKY received a B.S. in chemistry from Rensselaer Polytechnic Institute, and an M.S. and Ph.D. in physical chemistry from the Pennsylvania State University. From 1957 to 1979, he was a member of General Electric's Space Sciences Laboratory, where he conducted research on the spectroscopy of high-temperature species, chemical kinetics, and chemical and metal vapor lasers. He joined APL in 1979 as part of the Research Center and was a program director at the National Science Foundation from 1993 to 1996 (IPA from APL). He retired from APL in September 1996 and is currently a consultant with the General Physics Corporation. His research interests include combustion and flame chemistry, spectroscopic and radiometric properties of materials, high-speed flow diagnostics, and beam surface interactions. His e-mail address is mj118@psu.edu.



DANIEL T. PRENDERGAST joined APL in 1985 and is a Senior Professional Staff engineer in the Electro-Optical Systems Group of the Air Defense Systems Department. He received a B.F.A. degree from the Columbus College of Art and Design in 1978 and a B.S. degree in electrical engineering from The Ohio State University in 1985. Since joining APL, Mr. Prendergast has worked on the optical test and evaluation of infrared missile seekers as well as calibrating and developing optical test facilities. He has also worked on calibrating and aligning optical systems on MSX and NEAR. His e-mail address is daniel.prendergast@jhuapl.edu.